Tianjin Daxue Xuebao (Ziran Kexue yu Gongcheng Jishu Ban)/
Journal of Tianjin University Science and Technology
ISSN (Online):0493-2137
E-Publication: Online Open Access
Vol: 57 Issue: 12:2024
DOI: 10.5281/zenodo.14551073

ENHANCING MIMO ANTENNA PERFORMANCE THROUGH INNOVATIVE DECOUPLING SOLUTIONS

AMER NASER
University of Al-Zahraa for Women, Kerbala, Iraq.

SAIF NADHIM GALIB
Iraqi Ministry of Interior, Baghdad, Iraq. Email: saifalsaidy100@gmail.com

ALI NADHIM GALIB
Iraqi Ministry of Interior, Baghdad, Iraq.

KAWTHER KANNAN SALIH
University of Al-Zahraa for Women, Kerbala, Iraq.

FATIMA ABD-ALRASOOL
University of Al-Zahraa for Women, Kerbala, Iraq.

Abstract

This paper introduces a compact multiple-input multiple-output (MIMO) antenna design tailored for 5G cellular applications. The proposed array comprises four identical, compact antenna elements designed to deliver extensive radiation coverage and support diverse functionalities. Each antenna element is based on a dual-polarized square-ring resonator, which is fed by two T-shaped feed lines and operates at a frequency of 3.5 GHz, making it suitable for the 5G frequency band. The paper highlights the significance of achieving optimal isolation between adjacent elements and presents straightforward yet effective decoupling techniques to address this. These techniques include the incorporation of Ten zigzag slots between the radiator and feeder, a T-shaped feed line, rectangular slots within the feeders, a defected ground plane, and the strategic arrangement of radiating elements at varying orientations. The designed antenna achieves a bandwidth of 600 MHz (ranging from 3.25-3.85 GHz) and exhibits high-gain radiation patterns with minimal envelope correlation coefficient (ECC) and total active reflection coefficient (TARC). Experimental measurements validate that the antenna's performance aligns closely with the anticipated characteristics, demonstrating its reliability for practical 5G applications.

Keywords: 5G, MIMO, Dual-polarized Antenna, Defected Ground Structures (DGS), Resonator Antenna, Smartphone.

1. INTRODUCTION

Driven by advantages such as very high speeds, lower latency, and outstanding reliability, the ongoing advancement of mobile communication technology has prompted researchers worldwide to take a growing interest in 5G mobile communication systems [1]. Additionally, factors like increased channel capacity, excellent spectrum efficiency, and significant connection density further highlight the importance of this technology [2]. In 5G terminals, antennas are designed to be highly efficient with a low profile, wide operational bandwidth, and excellent mutual coupling properties, particularly for hand-held devices [3]. Microstrip antennas are ideal for cellular applications due to their cost-effectiveness and ease of integration, making them especially advantageous given the limited space available on smartphone boards [4]. Compact microstrip-fed printed

Tianjin Daxue Xuebao (Ziran Kexue yu Gongcheng Jishu Ban)/
Journal of Tianjin University Science and Technology
ISSN (Online):0493-2137
E-Publication: Online Open Access
Vol: 57 Issue: 12:2024
DOI: 10.5281/zenodo.14551073

antennas are particularly promising for smartphones due to their flat design, simple structure, and ease of integration with RF circuits, which help overcome the limitations on antenna size imposed by smartphone boards [5]. Recently, several designs for smartphone antennas targeting 5G applications have been proposed, focusing mainly on frequency ranges below 6 GHz [6]. However, many of these designs use single-polarized resonators, which occupy significant space on the non-planar mainboard structure, leading to restricted and poor radiation coverage. An innovative eight-port, four-element antenna design offers extensive radiation coverage and compact radiators [7]. Zigzag slots are used to enhance radiation efficiency and broaden the frequency range, but they may increase the likelihood of signal loss if not precisely fabricated. The T-shaped feed line improves power distribution but can complicate achieving proper matching between the feeder and the radiator. Rectangular slots enhance power flow but may lead to unwanted reflections. The defected ground plane reduces interference but can cause uneven power distribution and undesirable reflections if not carefully designed. Arranging radiating elements at different angles enhances directivity but can make controlling the radiation pattern more challenging.

In comparison to these methods, this research introduces an innovative approach that integrates all these techniques—slots between the radiator and feeder, a T-shaped feed line, rectangular slots within the feeder, a defected ground plane, and the strategic arrangement of radiating elements at varying orientations. By combining these techniques, a multi-layered defense against mutual coupling is created, with each technique addressing different aspects of electromagnetic interaction between antenna elements. This integrated approach results in a more comprehensive reduction in mutual coupling than any single method could achieve alone, clearly distinguishing the proposed approach from conventional methods and underscoring the significance of this work in antenna design. The proposed antenna design, optimized for a frequency of 3.7 GHz within the sub-6 GHz range of the 5G spectrum, was developed using the CST software suite [8]. The proposed MIMO architecture was also implemented, and its performance was rigorously evaluated through measurements [9]. To verify the accuracy of the antenna's performance, measurement data were compared with electromagnetic simulations [10]. Unlike previously developed MIMO antennas, our design offers notable characteristics such as excellent isolation, extensive radiation coverage, minimal ECC, TARC, and good signal integrity [11]. Moreover, channel capacity loss (CCL) is crucial as it directly impacts the efficiency of data transmission. The proposed design addresses this by optimizing the antenna structure to enhance channel capacity and reduce losses [12]. The following sections provide a detailed explanation of the key attributes of each radiator and the overall array design [13].

This paper is structured into four main sections. The first section provides a comprehensive introduction that outlines the importance of the research and the need for improvements in antenna design. The second section presents the research idea and applies it to a 2x2 MIMO antenna, including detailed calculations and performance analysis. In the third section, we scale up the design to an 8x8 MIMO configuration aimed at enhancing performance for 5G mobile phones, and we conduct thorough testing on

Tianjin Daxue Xuebao (Ziran Kexue yu Gongcheng Jishu Ban)/
Journal of Tianjin University Science and Technology
ISSN (Online):0493-2137
E-Publication: Online Open Access
Vol: 57 Issue: 12:2024
DOI: 10.5281/zenodo.14551073

this antenna to evaluate its performance. Finally, the fourth section summarizes the key findings and offers recommendations for future work.

2. SINGLE-ELEMENT ANTENNA

Figure 1 shows the suggested design schematic. A square-ring resonator is present on the top layer of the antenna configuration, accompanied by a pair of T-shape feed lines. Additionally**,** sixteen zigzag slots between the square ring and T-shape feed line, a square slot on the bottom layer of the antenna (DGS), and rectangular slots in the feed line to minimize the mutual coupling that could occur between the ports of the antenna. The proposed design was printed on an FR4 insulating substrate with relative loss (δ=0.025) and transmittance (ε=4.4), which is of thickness 1.6 mm.

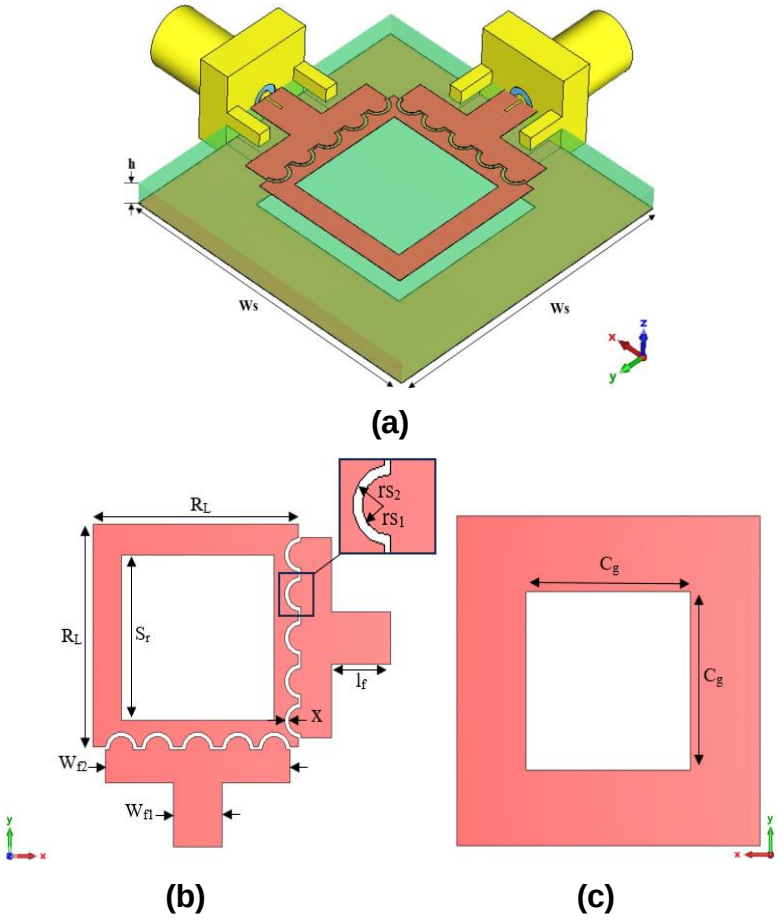

Figure 1: (a) Side-view (b) front-layer, and (c) back-layer of the Proposed Antenna Element

The modifications depicted in the attached image showcase the progression of the antenna design through four stages, as shown in Figure 2(a). In the initial stage (Ant. A), the design features a square resonator fed by a T-shaped feed line, with no alterations to the ground plane. This basic configuration serves as the foundation for further improvements. In the

Tianjin Daxue Xuebao (Ziran Kexue yu Gongcheng Jishu Ban)/
Journal of Tianjin University Science and Technology
ISSN (Online):0493-2137
E-Publication: Online Open Access
Vol: 57 Issue: 12:2024
DOI: 10.5281/zenodo.14551073

second stage (Ant. B), the design is updated by replacing the square resonator with a square-ring resonator, which enhances the antenna's radiation efficiency and broadens its operating bandwidth. The third stage (Ant. C) introduces a square slot in the ground plane beneath the resonator, which alters the current distribution on the ground plane, affects the resonant frequencies, and reduces unwanted modes. This modification also improves impedance matching, leading to more stable operation across a wider frequency range. The final stage (Ant. D) incorporates zigzag slots between the square-ring resonator and the T-shaped feed line. This modification not only enhances the feed elements but also optimizes the current path, minimizing interference between the resonators, and leading to improved antenna performance. The inclusion of zigzag slots also contributes to enhanced polarization purity and better signal isolation. Figure 2(b) illustrates the S-parameters (S11 and S12) for each design stage, showing how each modification contributes to an improved frequency response and overall performance. These results confirm that each step of refinement brings the design closer to optimal performance, particularly in terms of minimizing reflection and maximizing transmission efficiency.

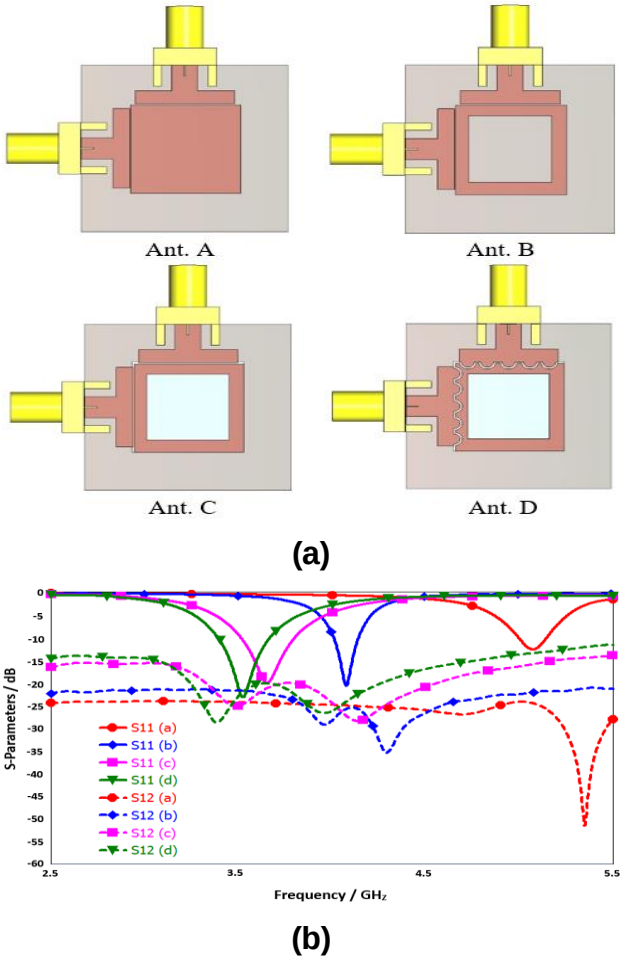

Figure 2: (A-D) Stages of development of the proposed antennas, and (b) S-parameter results

Tianjin Daxue Xuebao (Ziran Kexue yu Gongcheng Jishu Ban)/
Journal of Tianjin University Science and Technology
ISSN (Online):0493-2137
E-Publication: Online Open Access
Vol: 57 Issue: 12:2024
DOI: 10.5281/zenodo.14551073

Table 1: The Parameter Values of the Proposed Design

Parameter	Value (mm)	Parameter	Value (mm)
Sr	9.5	W_{f1}	3
R_L	12.75	W_{f2}	11.5
X	0.25	r_{s1}	0.75
C_G	15	rs_2	1
W_S	22	$L_{s\ MIMO}$	140
L_f	3.7	$W_{s\ MIMO}$	70

The design of the square-ring resonator antenna is influenced by several critical factors that significantly impact its performance, particularly in terms of the operating frequency range, reflection coefficient, and mutual coupling.

Figure 3.15 provides a detailed analysis of the S-parameters (S11 and S12) of the antenna across different values of key design parameters, including the feed line length (L_f), the side length of the inner square-ring resonator (S_r), the zigzag space between the square-ring resonator and the T-shaped feed line (X), and the square slot in the ground plane (C_g).

In Figure 3(a), the variations in S11 and S21 characteristics are examined for different values of L_f. It is observed that an L_f of 3.7 mm enhances the antenna's return losses, suggesting this as the optimal length for improved performance. Figure 3(b) illustrates the impact of varying the S_r dimensions, showing that an aperture size of S_r = 9.5 mm is the most favorable, resulting in the best overall performance in terms of resonance and efficiency. Figure 3(c) highlights the effect of changing the X parameter on the antenna's resonance frequency, with an X value of 0.25 mm yielding a resonance frequency of approximately 3.5 GHz. This emphasizes the crucial role of this parameter in fine-tuning the antenna's performance. Finally, Figure 3 (d) demonstrates the performance of the S-parameter for different values of C_g. A C_g value of 15 mm strikes a balance between achieving optimal resistance bandwidth and maintaining sufficient isolation between the resonator and

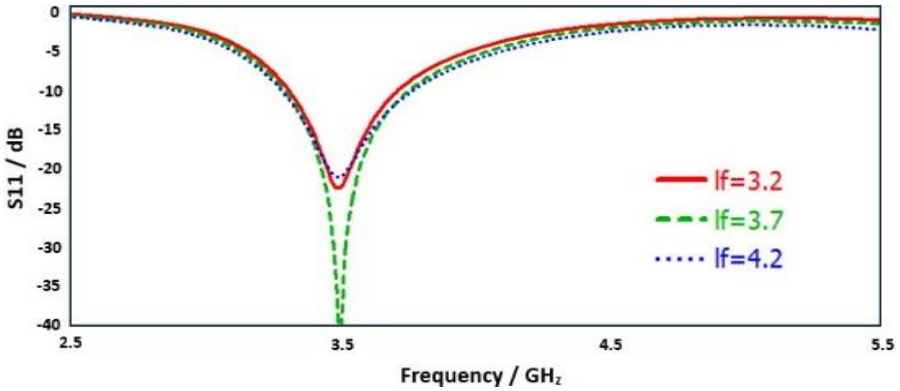

(a)

Tianjin Daxue Xuebao (Ziran Kexue yu Gongcheng Jishu Ban)/
Journal of Tianjin University Science and Technology
ISSN (Online):0493-2137
E-Publication: Online Open Access
Vol: 57 Issue: 12:2024
DOI: 10.5281/zenodo.14551073

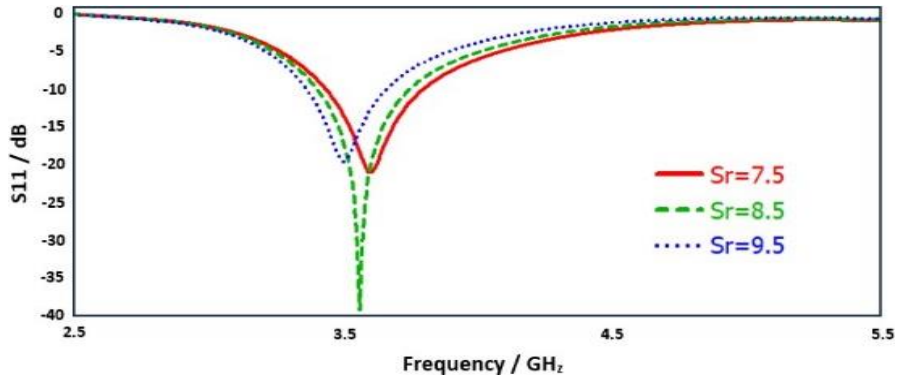

(b)

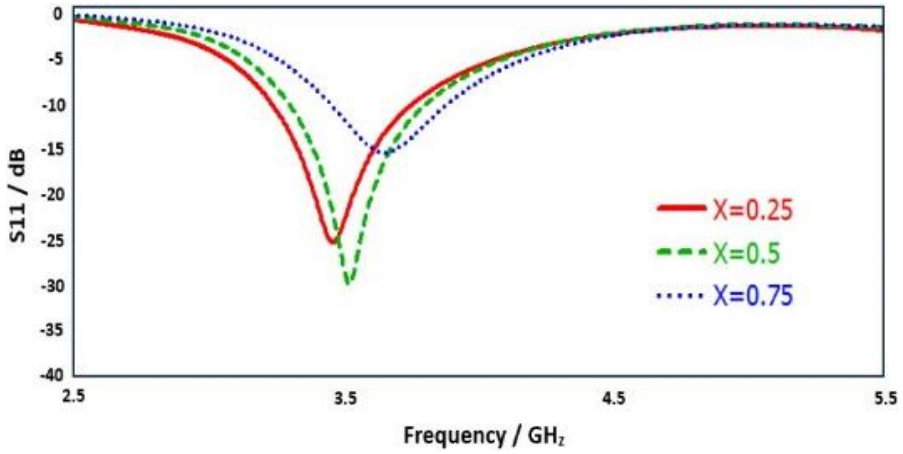

(c)

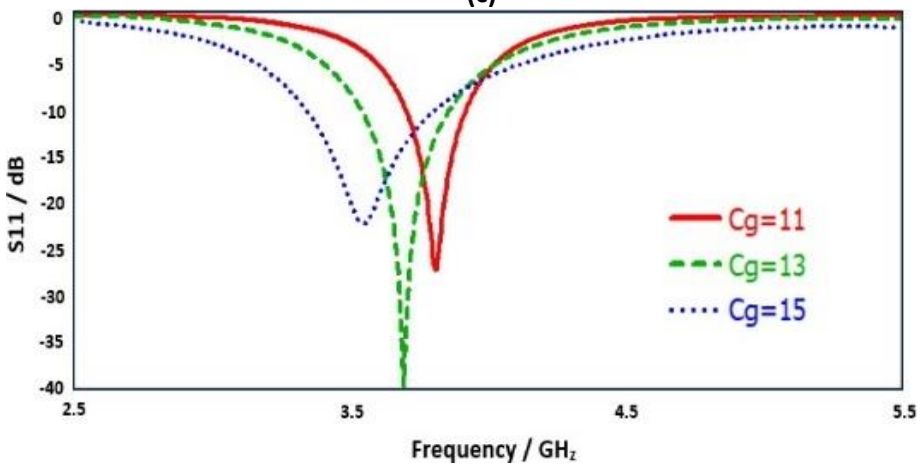

(d)

Figure 3: S11 and S12 results of the antenna for various values of (a) lf, (b) Sr, (c) X, (d) Cg

Feed line, which is crucial for minimizing unwanted signal interference.

Tianjin Daxue Xuebao (Ziran Kexue yu Gongcheng Jishu Ban)/
Journal of Tianjin University Science and Technology
ISSN (Online):0493-2137
E-Publication: Online Open Access
Vol: 57 Issue: 12:2024
DOI: 10.5281/zenodo.14551073

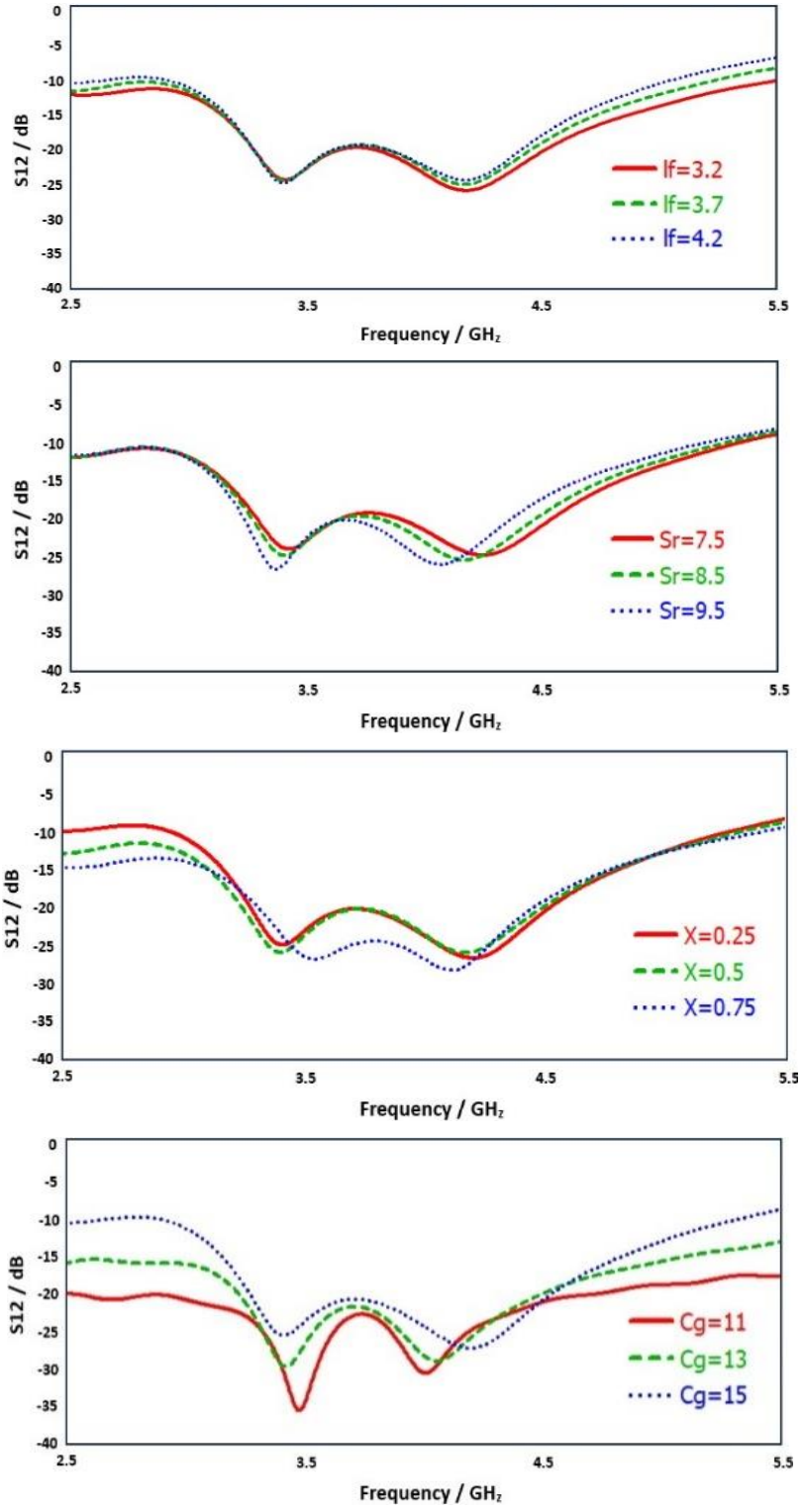

The performance of the zigzag edge square ring resonator antenna was analyzed, focusing on key parameters such as return loss and isolation, as illustrated in Figure 4. At a

Tianjin Daxue Xuebao (Ziran Kexue yu Gongcheng Jishu Ban)/
Journal of Tianjin University Science and Technology
ISSN (Online):0493-2137
E-Publication: Online Open Access
Vol: 57 Issue: 12:2024
DOI: 10.5281/zenodo.14551073

resonance frequency of 3.5 GHz, the antenna exhibits an S11 value of -23 dB. This resonator covers a bandwidth of 300 MHz, from 3.37 GHz to 3.67 GHz, at a -10 dB return loss. Additionally, the antenna extends its bandwidth to 800 MHz, ranging from 3.25 GHz to 3.85 GHz, at a -6 dB return loss. The mutual coupling between the antenna elements is impressively low, measured at approximately -23 dB at the resonance frequency. The selection of this frequency for 5G applications is particularly beneficial due to its optimal balance between coverage, capacity, and penetration through obstacles, all while maintaining high data transmission speeds.

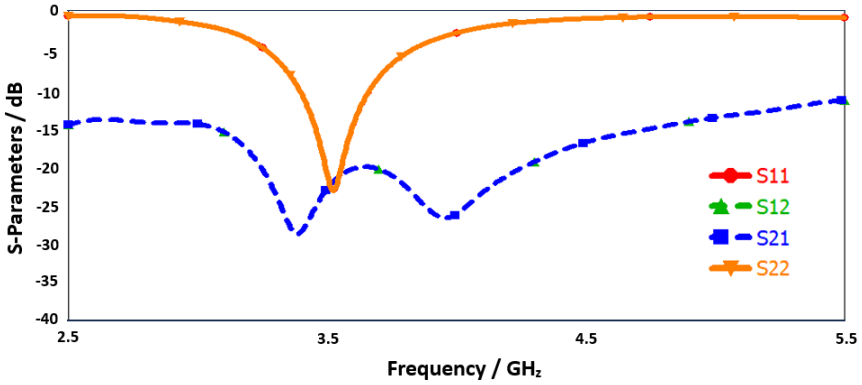

Figure 4: S-Parameter of single antenna element

As previously mentioned, analyzing the current distribution is essential for assessing the efficiency and performance of resonant antennas, as it significantly influences both radiation power and signal transmission. Figure 5 presents the current distribution of the designed antenna at the resonant frequency of 3.5 GHz, with excitation from both ports 1 and 2. The results indicate that the current is strategically concentrated in the zigzag regions surrounding the resonator and in the lower slot at the base. These slots play a critical role in mitigating surface currents, thereby improving the overall performance of the antenna [14, 15].

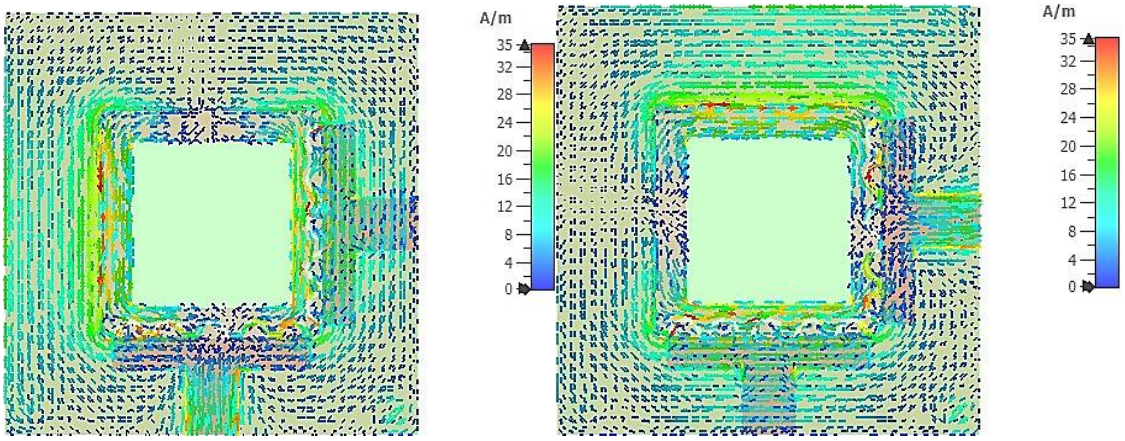

Port 1 **Port 2**

Figure 5: Current distribution at 3.5 GHz for port 1 and port 2

Tianjin Daxue Xuebao (Ziran Kexue yu Gongcheng Jishu Ban)/
Journal of Tianjin University Science and Technology
ISSN (Online):0493-2137
E-Publication: Online Open Access
Vol: 57 Issue: 12:2024
DOI: 10.5281/zenodo.14551073

Figure 6 depicts the 3D radiation pattern of the proposed antenna under varying feeding conditions (Port 1 and Port 2) at a resonant frequency of 3.5 GHz. The determination of an antenna's 3D radiation pattern is critical for understanding its energy distribution, directivity, and the potential for interference within antenna systems. A thorough analysis of these patterns is vital for optimizing the design of multi-antenna systems and enhancing their performance. The proposed antenna demonstrates consistent radiation patterns under the examined feeding conditions, featuring orthogonal polarizations and a gain exceeding 3.5 dB. The radiation pattern is predominantly quasi-spherical or omnidirectional, which ensures uniform signal coverage across all directions, contributing to its overall efficiency in various applications.

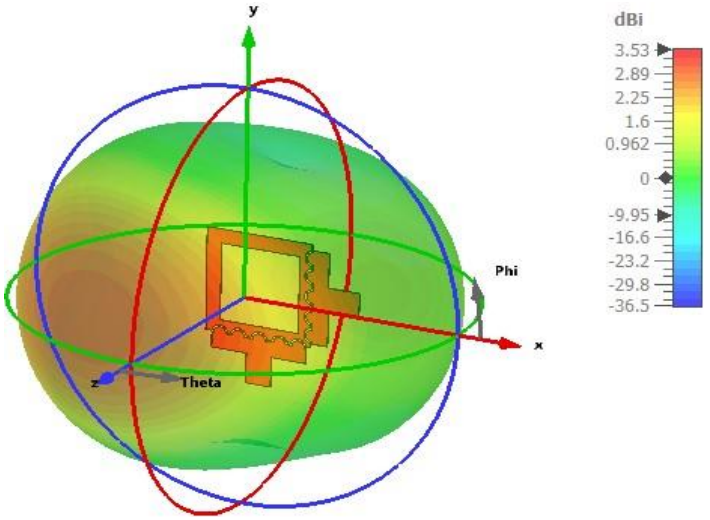

Port1

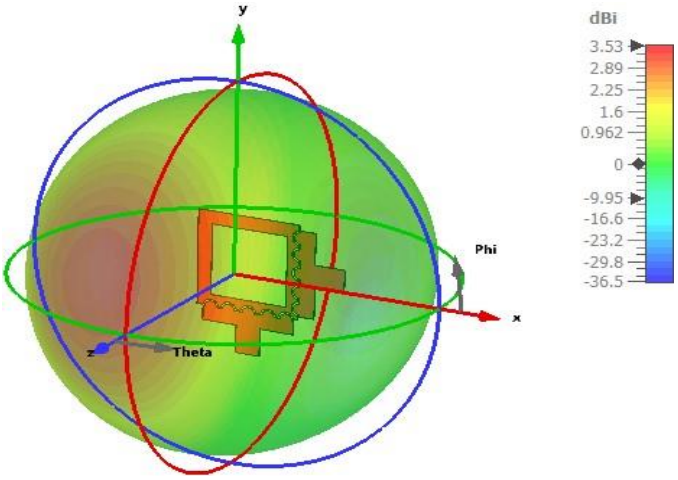

Port2

Figure 6: 3D radiation patterns of the proposed antenna at 3.5 GHz for port 1, and port 2

Tianjin Daxue Xuebao (Ziran Kexue yu Gongcheng Jishu Ban)/
Journal of Tianjin University Science and Technology
ISSN (Online):0493-2137
E-Publication: Online Open Access
Vol: 57 Issue: 12:2024
DOI: 10.5281/zenodo.14551073

The efficiency characteristics and maximum gain results of the proposed design are shown in Figure 7. The figure reveals a high radiation efficiency exceeding 87%, and the design demonstrates an overall efficiency greater than 75% across the required frequency range. Furthermore, the maximum gain of the antenna ranges from 3.5 to 3.8 dBi.

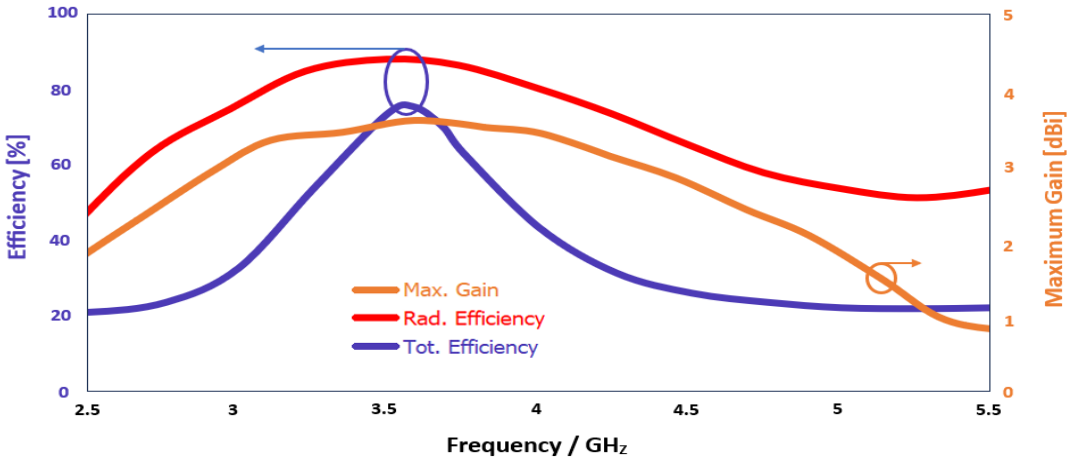

Figure 7: Efficiencies, and maximum gain for single-element antenna

3. THE PROPOSED MIMO 5G SMARTPHONE ANTENNA

The proposed 8x8 MIMO antenna operates at a frequency of 3.5 GHz and consists of integrating four 2x2 MIMO antenna arrays (following the same design principles outlined in Figure 8) positioned at the corners of the PCB. This configuration makes it particularly well-suited for 5G applications. The selected frequency is ideal for meeting the requirements of 5G communications, with the proposed antenna proving its efficiency in delivering high-speed data and low-latency connections. The antenna feed lines are arranged perpendicularly to achieve orthogonal polarization, enhancing isolation and the overall performance of the antenna. The innovative design features square-ring resonators with zigzag edges and a slotted ground plane. The antenna is designed on an FR-4 substrate, with dimensions of) 140× 70× 1.6)mm³. The compact size of this antenna system was achieved by utilizing small-sized single antenna elements, allowing the overall design to remain space-efficient. The use of small antenna elements not only allows for a more compact layout but also helps in improving radiation efficiency by reducing losses associated with larger arrays. Integrating these antenna arrays into the MIMO system offers numerous benefits, including increased efficiency, improved signal strength, and reduced losses. Additionally, the design is more compact, conserving space an important factor for applications that require multiple antennas in a confined area, such as mobile devices. This compactness is crucial for modern 5G devices, which require high-performance antennas within limited space, ensuring optimal communication without compromising on size. Figure 3.16 offers a comprehensive overview of the proposed MIMO antenna design. Figure 8(a) presents a side view, highlighting the basic parameters and port distribution, while Figures 8(b) and 8(c) display the front and rear views of the proposed antenna design, respectively.

Tianjin Daxue Xuebao (Ziran Kexue yu Gongcheng Jishu Ban)/
Journal of Tianjin University Science and Technology
ISSN (Online):0493-2137
E-Publication: Online Open Access
Vol: 57 Issue: 12:2024
DOI: 10.5281/zenodo.14551073

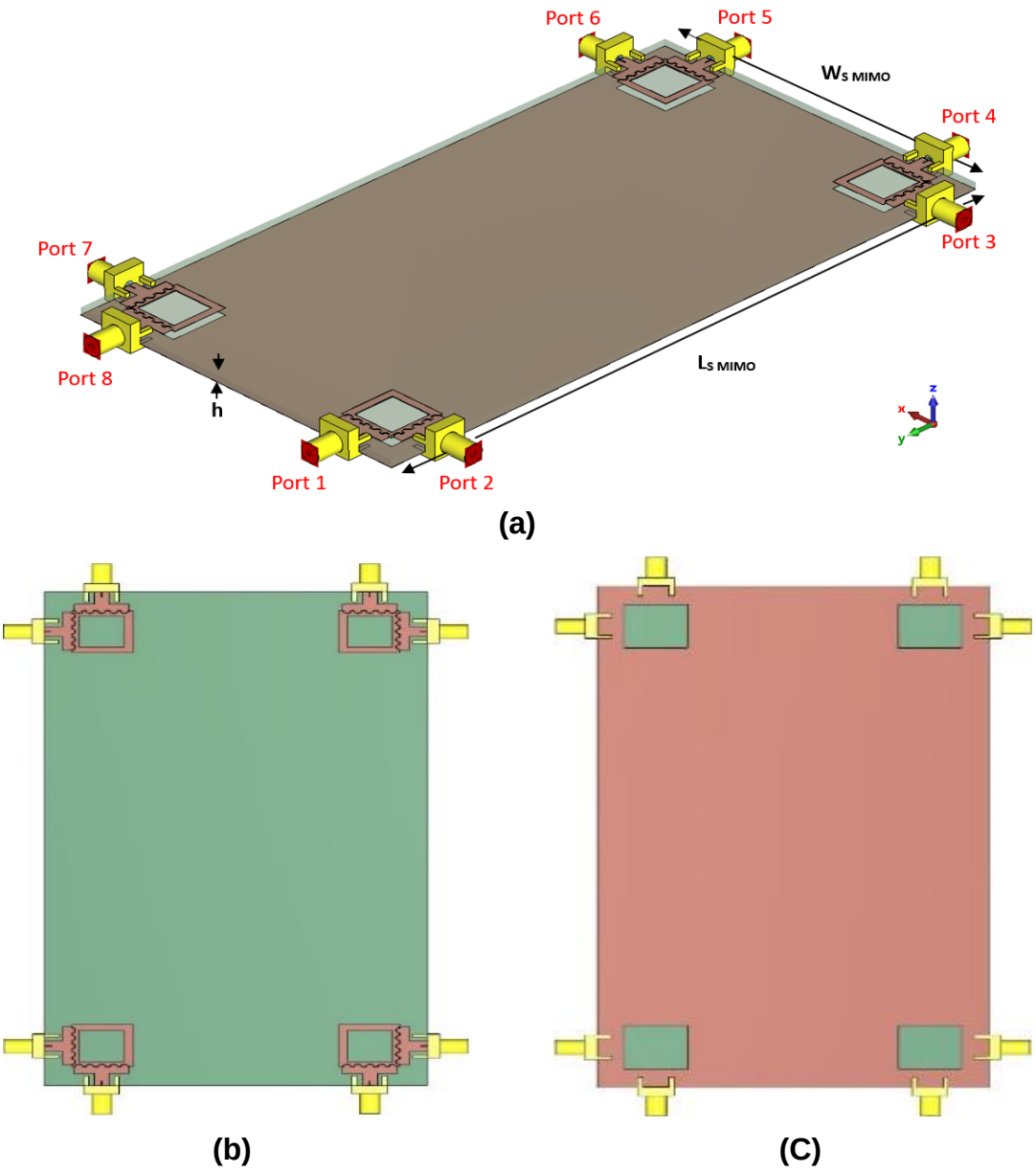

Figure 8: (a) Side-view (b) front-layer, and (c) back-layer of the proposed MIMO antenna design

After integrating four single-element square-ring resonator antennas at the edges of the PCB, the performance of the MIMO antenna was evaluated, as shown in Figure 9(a). The radiation elements of the MIMO antenna maintain return loss characteristics similar to those of the individual single-element antennas, with minor variations due to their close proximity in a confined space.

This design achieves excellent impedance matching, evidenced by reflection coefficients around -21 dB at 3.5 GHz. Additionally, the mutual coupling between the antenna

Tianjin Daxue Xuebao (Ziran Kexue yu Gongcheng Jishu Ban)/
Journal of Tianjin University Science and Technology
ISSN (Online):0493-2137
E-Publication: Online Open Access
Vol: 57 Issue: 12:2024
DOI: 10.5281/zenodo.14551073

elements is kept below -21 dB, as illustrated in Figure 9(b). This low level of mutual coupling is crucial in preventing significant degradation in radiation performance, making the antenna design particularly well-suited for 5G smartphone applications.

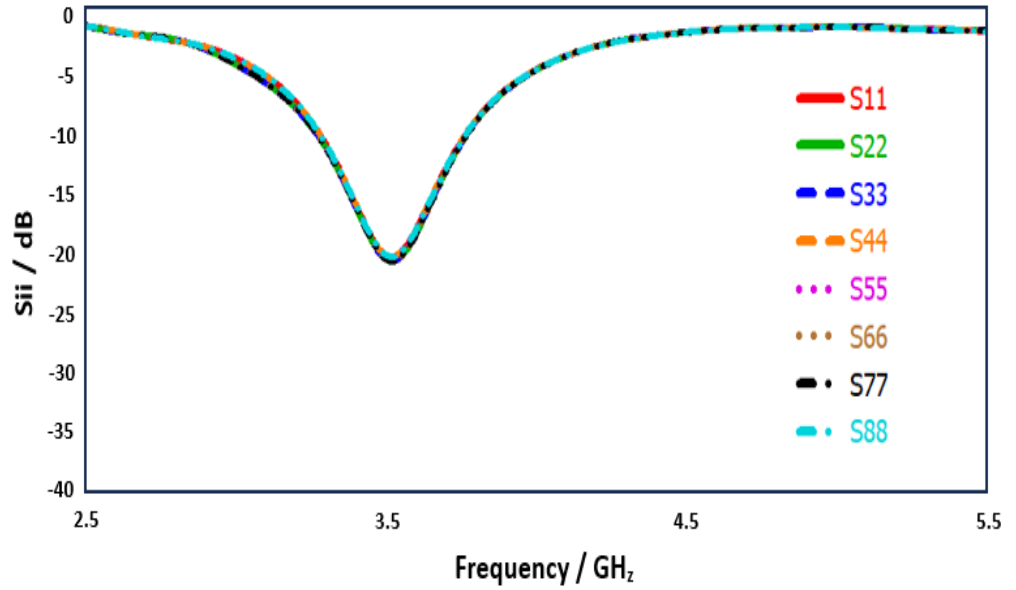

(a)

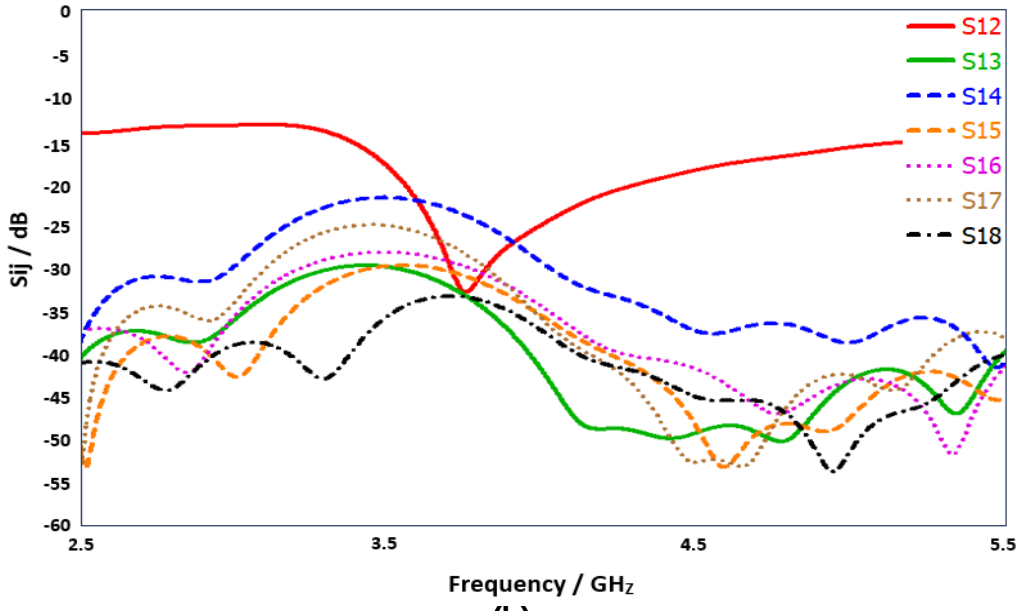

(b)

Figure 9: S-parameter results for MIMO antenna, (a) Sii and (b) Sij

Figure 10 shows two types of efficiencies: radiation efficiency and total efficiency, over the frequency range from 2.5 to 5.5 GHz. The figure indicates that radiation efficiency reaches 82% at the resonant frequency of 3.5 GHz, while total efficiency peaks at 70% at the same frequency.

Tianjin Daxue Xuebao (Ziran Kexue yu Gongcheng Jishu Ban)/
Journal of Tianjin University Science and Technology
ISSN (Online):0493-2137
E-Publication: Online Open Access
Vol: 57 Issue: 12:2024
DOI: 10.5281/zenodo.14551073

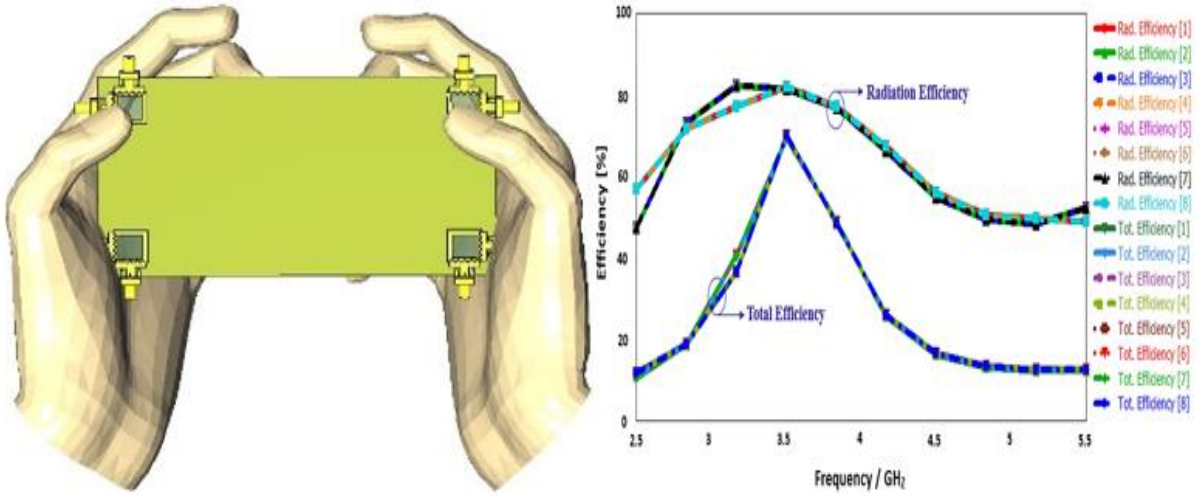

Figure 10: Efficiencies of the MIMO antenna in use mode

The envelope correlation coefficient (ECC) and the total active reflection coefficient (TARC) for the proposed design are shown in Figures 11(a) and (b). These characteristics can be calculated from the S-parameter results using the formulas Eq. (1) and Eq. (2). The ECC remains below 0.02 across the entire bandwidth, indicating minimal correlation between adjacent elements. At 3.5 GHz, the TARC value is less than -23, demonstrating the antenna's suitability for MIMO applications [16].

$$ECC = \frac{|Sjj* Sji+Sij* Sii|^2}{(1-|Sjj|^2-|Sji|^2)(1-|Sij|^2-|Sii|^2)}\ dB \quad (1)$$

$$TARC = \sqrt{\frac{(Sjj+Sji)^2+(Sij+Sii)^2}{2}}\ dB \quad (2)$$

where, Sii and Sjj are the return losses, Sij and Sji are the mutual coupling.

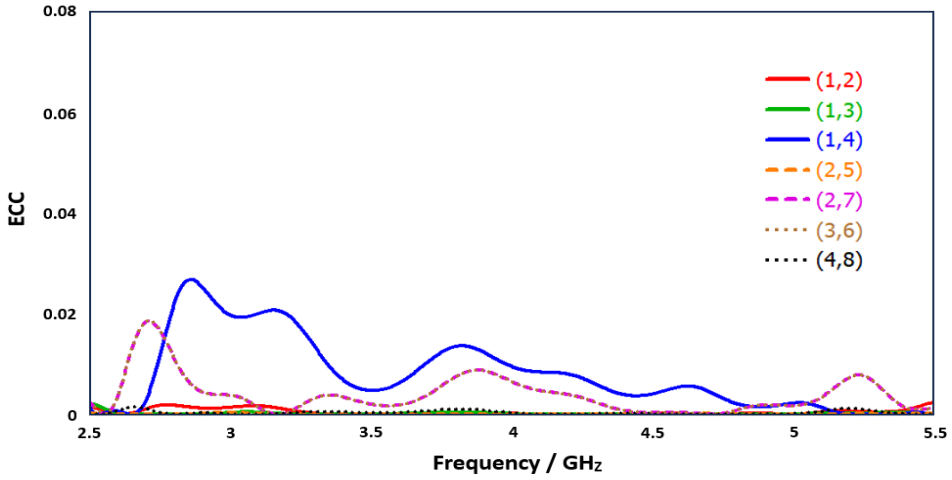

(a)

Tianjin Daxue Xuebao (Ziran Kexue yu Gongcheng Jishu Ban)/
Journal of Tianjin University Science and Technology
ISSN (Online):0493-2137
E-Publication: Online Open Access
Vol: 57 Issue: 12:2024
DOI: 10.5281/zenodo.14551073

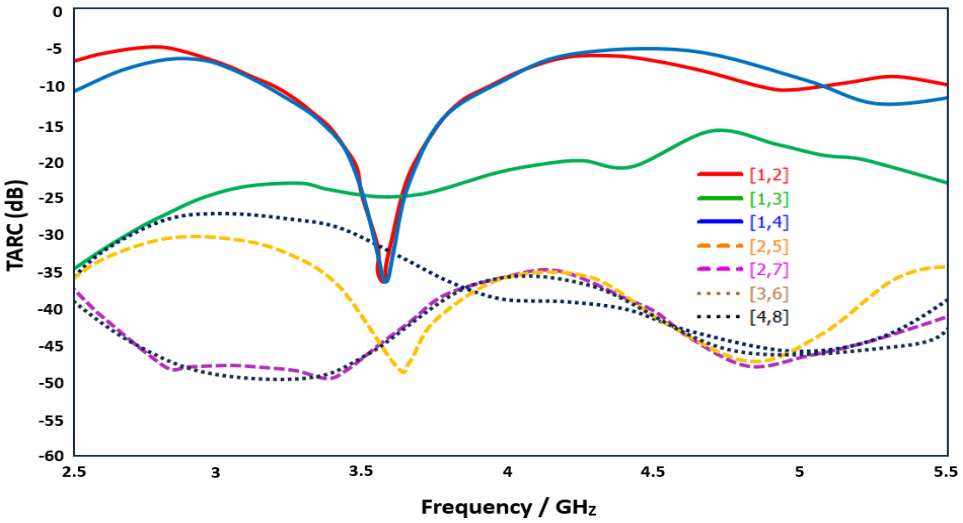

(b)

Figure 11: Simulated MIMO antenna, (a) (ECC), and (b) (TARC)

The 3D radiation pattern evaluation is essential to visualize the power distribution and directivity, and to identify potential interference within the MIMO antenna systems integrated on the 5G smartphone PCB.

These radiation patterns reveal that the radiators provide comprehensive coverage of all sides of the smartphone PCB, ensuring consistent signal transmission and reception. Figure 12 shows the consistent radiation patterns of the antenna at 3.5 GHz under various feeding conditions (Port 1 - Port 8), each of which exhibits orthogonal polarizations.

The antenna achieves a gain of around (5.8-7.5) dBi.

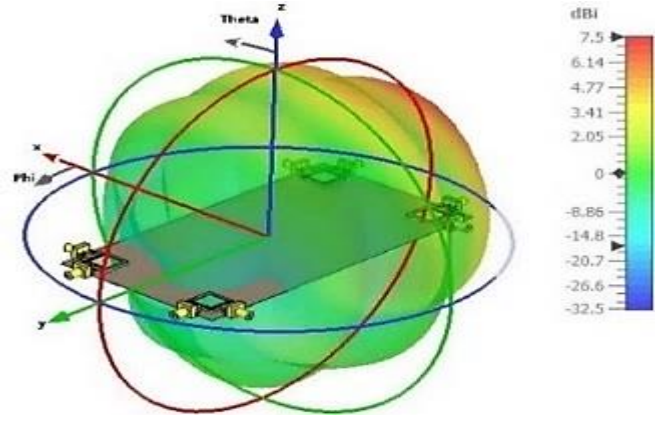

(a)

Tianjin Daxue Xuebao (Ziran Kexue yu Gongcheng Jishu Ban)/
Journal of Tianjin University Science and Technology
ISSN (Online):0493-2137
E-Publication: Online Open Access
Vol: 57 Issue: 12:2024
DOI: 10.5281/zenodo.14551073

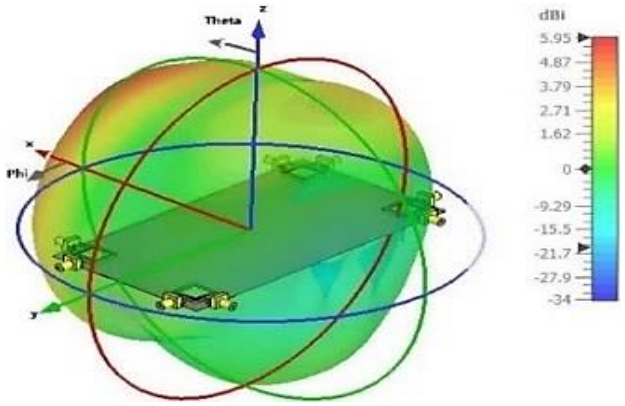

(b)

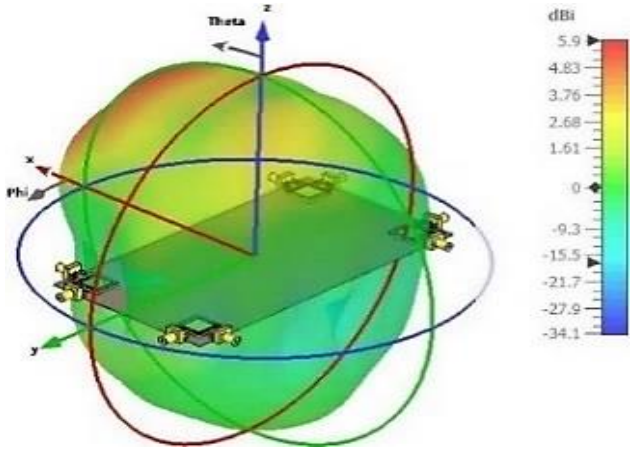

(c)

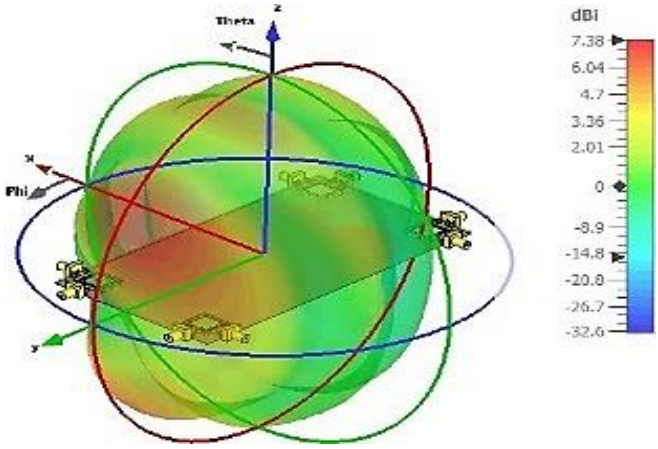

(d)

Figure 12: 3D radiation patterns for the 8 antenna elements at 3.4 GHz (a) antenna 1, (b) antenna 2, (c) antenna 3, (d) antenna 4, (a) antenna 5, (b) antenna 6, (c) antenna 7, and (d) antenna 8

Tianjin Daxue Xuebao (Ziran Kexue yu Gongcheng Jishu Ban)/
Journal of Tianjin University Science and Technology
ISSN (Online):0493-2137
E-Publication: Online Open Access
Vol: 57 Issue: 12:2024
DOI: 10.5281/zenodo.14551073

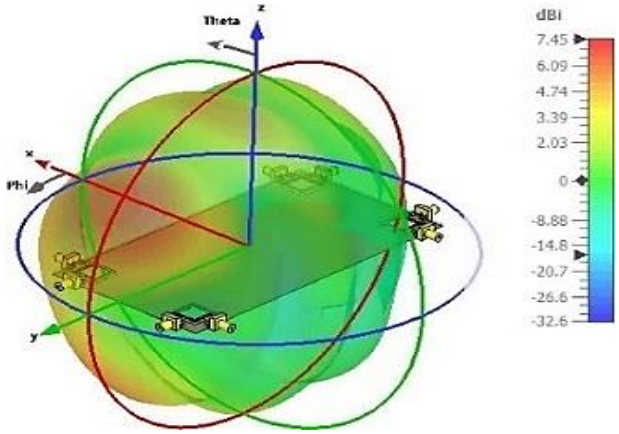

(e)

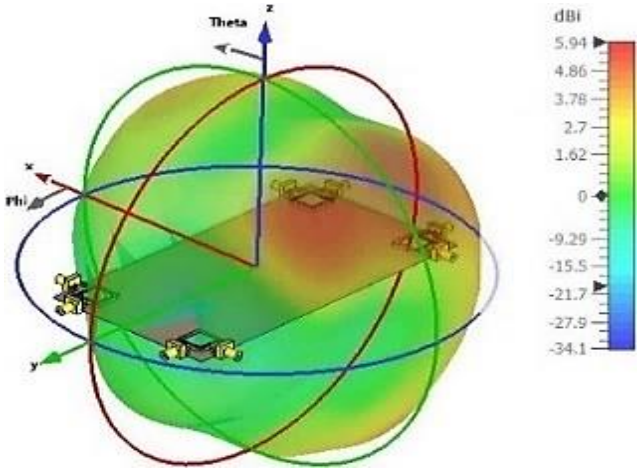

(f)

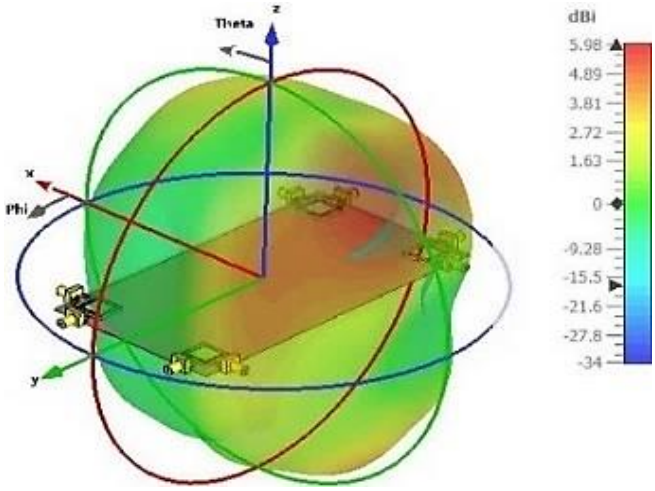

(g)

Tianjin Daxue Xuebao (Ziran Kexue yu Gongcheng Jishu Ban)/
Journal of Tianjin University Science and Technology
ISSN (Online):0493-2137
E-Publication: Online Open Access
Vol: 57 Issue: 12:2024
DOI: 10.5281/zenodo.14551073

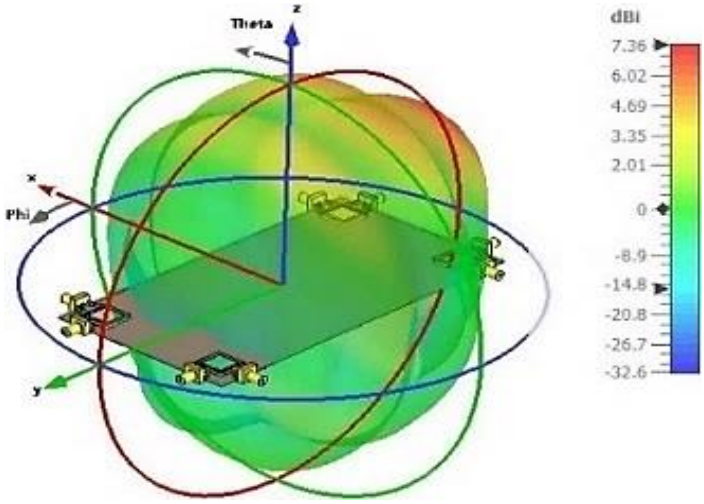

Another critical parameter for evaluating the MIMO performance of a multi-antenna design is the channel capacity loss (CCL), which arises from the mutual correlation between antenna elements in MIMO systems.

The degradation in system performance can be quantified by the capacity loss. The CCL in a MIMO system is primarily influenced by the S-parameters. For an 8 × 8 MIMO system, the CCL can be calculated using the formulas described below. It is important to note that the acceptable limit for CCL is ≤0.4 bps/Hz [16].

$$CCL = \log_2 \det(\Psi^{SNR}) \qquad bps/Hz \tag{3}$$

where the Ψ^{SNR} is the channel SNR determined as:

where

$$\Psi^{SNR} = \begin{bmatrix} p_{ii} & \cdots & p_{ij} \\ \vdots & \ddots & \vdots \\ p_{ji} & \cdots & p_{jj} \end{bmatrix}$$

$$p_{ii} = 1 - (|s_{ii}|^2 + |s_{ij}|^2)$$

$$p_{ij} = -(s_{ii} * s_{ij} + s_{ji} * s_{ij}) \tag{4}$$

Figure 13 illustrates the CCL value for the proposed MIMO antenna, demonstrating that the design exhibits extremely low channel capacity loss across the entire operational bandwidth, within the frequency range of 2.5 to 5.5 GHz.

It is observed that the CCL value remains below the acceptable threshold of 0.4 bits per second per hertz, indicating strong performance with minimal channel capacity loss throughout this spectrum.

Tianjin Daxue Xuebao (Ziran Kexue yu Gongcheng Jishu Ban)/
Journal of Tianjin University Science and Technology
ISSN (Online):0493-2137
E-Publication: Online Open Access
Vol: 57 Issue: 12:2024
DOI: 10.5281/zenodo.14551073

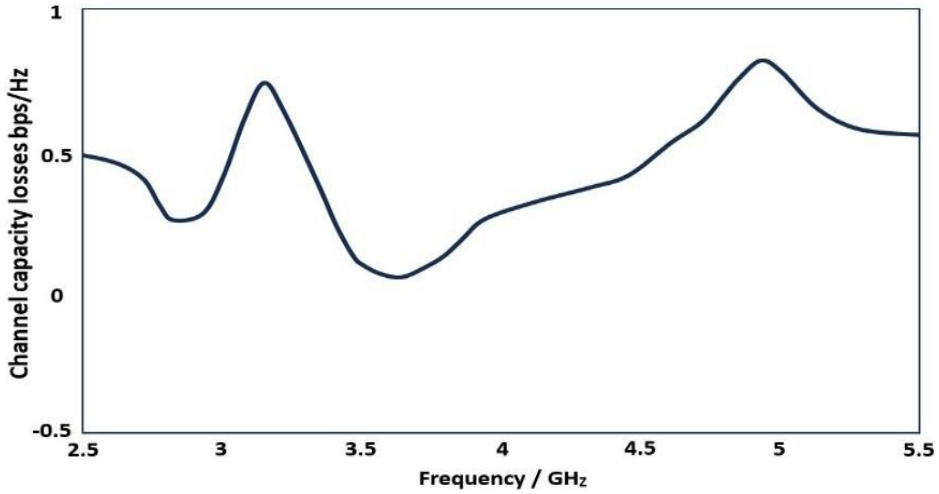

Figure 13: CCL of the MIMO Proposed Antenna

Figure 14 presents the analysis of Diversity Gain (DG), which clearly demonstrates that all ports exhibit a DG greater than 9.8 dB. This high DG value confirms the effectiveness of the antenna element diversity, ensuring superior performance and quality in the system.

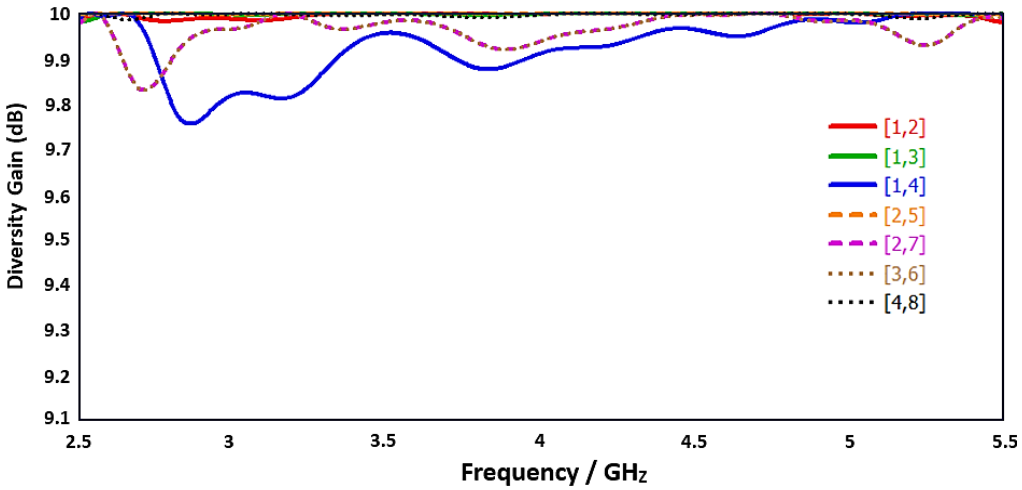

Figure 14: Diversity gain of the MIMO antenna proposed design

Transparent views of the 3D radiation patterns in the Talk-Mode scenario for each radiation element at 3.5 GHz are represented in Figure 3.36. Overall, the design provides sufficient radiation coverage and appropriate gain values for each square-ring resonator located at the corners of the PCB in the smartphone. The radiation performance of the diversity antenna depends on its location and distance from the human body. The antenna gain ranges from 4.7 to 7.2 dBi.

Tianjin Daxue Xuebao (Ziran Kexue yu Gongcheng Jishu Ban)/
Journal of Tianjin University Science and Technology
ISSN (Online):0493-2137
E-Publication: Online Open Access
Vol: 57 Issue: 12:2024
DOI: 10.5281/zenodo.14551073

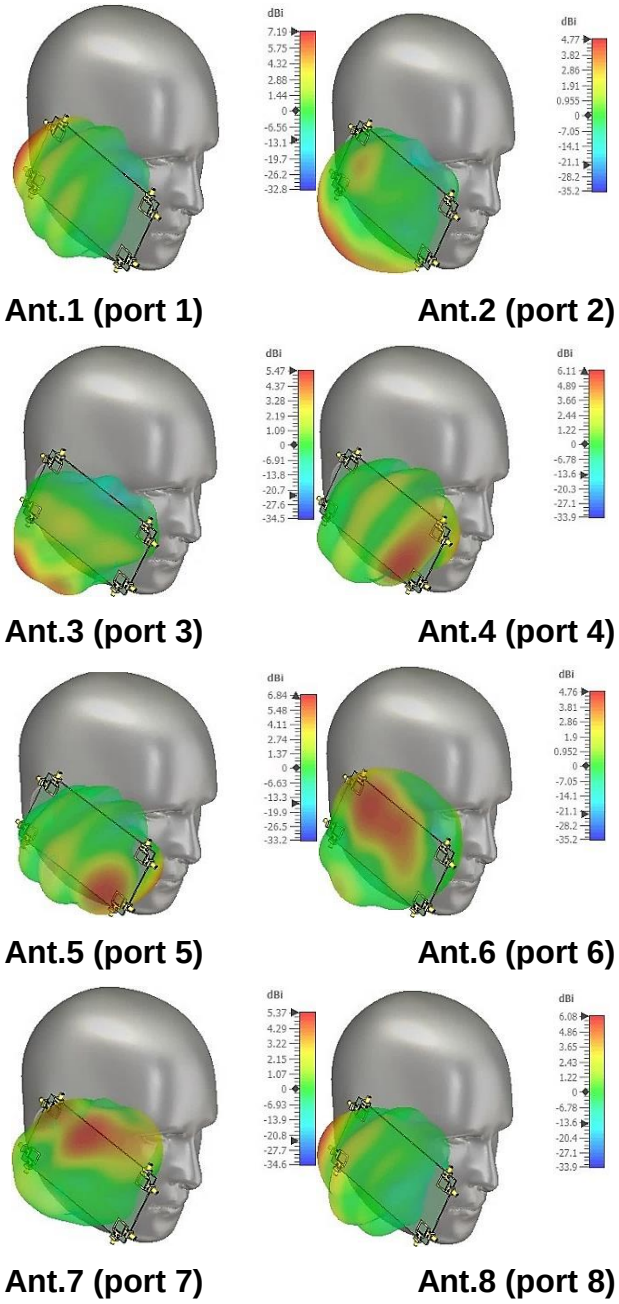

Figure 15: The radiation pattern of the antenna elements in use mode for (port1-port8)

Table 2 presents a comparative analysis of the proposed antenna with existing designs, focusing on key parameters such as the number of antenna elements, bandwidth, efficiency, size, isolation, ECC, CCL, and gain. The proposed antenna demonstrates a significantly broader bandwidth of 2.5-5.5 GHz and superior isolation of -21 dB,

Tianjin Daxue Xuebao (Ziran Kexue yu Gongcheng Jishu Ban)/
Journal of Tianjin University Science and Technology
ISSN (Online):0493-2137
E-Publication: Online Open Access
Vol: 57 Issue: 12:2024
DOI: 10.5281/zenodo.14551073

outperforming other designs. With an efficiency range of 65-70% and a compact footprint of 140x70 mm², it is well-suited for 5G applications. Additionally,

Table 2: Comparisons of a proposed antenna with recently released MIMO antennas

Ref.	Antenna elements	B.W (GHz)	Effi. (%)	Size (mm^2)	Iso. (Sij) (dB)	ECC	Gain dBi
[17]	8x8	3.4-3.6 (-6dB)	40-52	150x75	>10	<0.15	NA
[18]	8x8	3.3-3.6	45-60	124x40	>15	<0.15	4.3
[19]	8x8	3.4-3.6 4.8-5.1 (-6dB)	41-72 40-85	150x75	>11.5	<0.08 <0.05	NA
[20]	8x8	3.55-3.65	48-58	136x68	>13	<0.2	NA
[21]	8x8	3.4-3.6	59-98	150x75	>19.1	<0.012	3.1
[22]	8x8	3.4-3.6	47-65	150x75	>12	<0.1	3.2
[23]	8x8	3.4-3.7 (-6dB)	50-75	136x68	>15	<0.1	4
[24]	8x8	3.4-3.65 (-6dB)	34-76	150x75	>21	<0.01	4.8
[25]	8 x 8	3.4-3.6 (-6dB)	>40	150x75	>10	<0.1	NA
This work	**2x2 &**	**3.25-3.85**	**70-75**	**22x22**	**23**	**<0.02**	**3.5-3.8**
	8x8	**3.3-3.8**	**65-70**	**140x75**	**21**		**5.9-7.5**

4. CONCLUSIONS

This manuscript presents an enhanced design for a resonator antenna aimed at optimizing 5G MIMO mobile terminals. The proposed configuration features an eight-port setup with four modified square-ring resonators positioned at the corners of the mobile phone mainboard. To minimize mutual coupling, the design incorporates ten zigzag slots between the radiators and feeders, a T-shaped feed line, a defected ground plane, and a strategic arrangement of radiating elements at varying orientations. The MIMO antenna design ensures comprehensive radiation coverage and supports dual polarization on both sides of the PCB, which is crucial for effective 5G communication.

The antenna's extremely low ECC (<0.02) highlights its excellent signal diversity, making it highly effective in minimizing interference and enhancing communication reliability in MIMO systems. It is crucial to highlight that many previous studies do not comprehensively address all essential metrics, such as efficiency and gain. This omission restricts the depth of their analysis and results in a less complete evaluation of MIMO antenna performance. The antenna was fabricated and tested, revealing a strong correlation between simulated and measured results. The radiators operate within a frequency range of 3.25 to 3.85 GHz for a single antenna element and 3.3 to 3.8 GHz for the MIMO antenna, with a resonance at 3.5 GHz. A thorough investigation was conducted into the critical aspects of the smartphone antenna design, including S-parameters, efficiency, radiation patterns, gain, ECC, TARC, and CCL results.

Tianjin Daxue Xuebao (Ziran Kexue yu Gongcheng Jishu Ban)/
Journal of Tianjin University Science and Technology
ISSN (Online):0493-2137
E-Publication: Online Open Access
Vol: 57 Issue: 12:2024
DOI: 10.5281/zenodo.14551073

References

1) A. Ren, Y. Liu, H. Yu, Y. Jia, C. Sim, and Y. Xu, "A High Isolation Building Block Using Stable Current Nulls for 5G Smartphone Applications," IEEE Access, vol. 60, pp. 170419–170429, 2019.

2) Z. Qin, W. Geyi, M. Zhang, and J. Wang, "Printed eight-element MIMO system for compact and thin 5G mobile handset," Electronics Letters, vol. 52, pp. 416–418, 2016.

3) K. Ming, H. Wahl, K. Man, and C. Hou, "Circularly Polarized Patch Antenna for Future 5G Mobile Phones," IEEE Access, vol. 2, pp. 1521–1529, 2014.

4) L. Song and J. Geng, "Analysis and Design of a Dual-polarized Printed Monopole Antenna," IETE Journal of Research, pp. 1-8, 2019.

5) N. Parchin, J. Zhang, R. Abd-Alhameed, G. Pedersen, and S. Zhang, "A Planar Dual-Polarized Phased Array with Broadband Width and Quasi-Endfire Radiation for 5G Mobile Handsets," IEEE Transactions on Antennas and Propagation, vol. 69, no. 10, pp. 6410–6419, 2021.

6) Y. Li, Y. Luo, and G. Yang, "High-isolation 3.5 GHz eight-antenna MIMO array using balanced open-slot antenna element for 5G smartphones," IEEE Transactions on Antennas and Propagation, vol. 67, pp. 3820–3830, 2019.

7) A. Ullah, N. Parchin, A. Amar, and R. Abd-Alhameed, "Phased Array Antenna Design with Improved Radiation Characteristics for Mobile Handset Applications," in Proceedings of the 16th European Conference on Antennas and Propagation (EuCAP), pp. 14, 2022.

8) Q. Lai, Y. Pan, and S. Zheng, "A Self-Decoupling Method for MIMO Antenna Array Using Characteristic Mode of Ground Plane," IEEE Transactions on Antennas and Propagation, vol. 71, no. 3, pp. 2126–2135, 2023.

9) M. Li, Z. Xu, Y. Ban, C. Sim, and Z. Yu, "Eight-port orthogonally dual-polarized MIMO antennas using loop structures for 5G smartphone," IET Microwaves, Antennas & Propagation, vol. 11, no. 12, pp. 1810–1816, 2017.

10) A. Zhao and Z. Ren, "Size reduction of self-isolated MIMO antenna system for 5G mobile phone applications," IEEE Antennas and Wireless Propagation Letters, vol. 18, pp. 152–156, 2018.

11) S. H. Kiani, A. Altaf, M. R. Anjum, S. Afridi, Z. A. Arain, S. Anwar, and E. Limit, "MIMO Antenna System for Modern 5G Handheld Devices with Healthcare and High Rate Delivery," Sensors, vol. 21, p. 7415, 2021.

12) H. Kiani, A. Altaf, M. Anjum, S. Afridi, Z. Arain, S. Anwar, S. Khan, M. Ali Bakhshikenari, A. Lalbakhsh, M. A. Khan, R. A. Abd-Alhameed, and E. Limiti, "MIMO Antenna System for Modern 5G Handheld Devices with Healthcare and High Rate Delivery," Sensors, vol. 21, no. 21, pp. 119, 2021.

13) K. Wong, C. Tsai, and J. Lu, "Two Asymmetrically Mirrored Gap-Coupled Loop Antennas as a Compact Building Block for Eight-Antenna MIMO Array in the Future Smartphone," IEEE Transactions on Antennas and Propagation, vol. 65, no. 4, pp. 1765–1778, 2017.

14) CST Microwave Studio, Version 2023, CST, Framingham, MA, USA, 2023.

15) M. Abdullah, A. Altaf, M. Anjum, Z. Arain, A. Jamali, M. Alibakhshikenari, F. Falcone, and E. Limiti, "Future smartphone: MIMO antenna system for 5G mobile terminals," IEEE Access, vol. 9, pp. 91593–91603, 2021.

16) S. Kiani, H. Savci, H. Abubakar, N. Parchin, H. Rimli, and B. Hakim, "Eight-Element MIMO Antenna Array with Tri-Band Response for Modern Smartphones," IEEE Access, vol. 11, pp. 44244–44253, 2023.

Tianjin Daxue Xuebao (Ziran Kexue yu Gongcheng Jishu Ban)/
Journal of Tianjin University Science and Technology
ISSN (Online):0493-2137
E-Publication: Online Open Access
Vol: 57 Issue: 12:2024
DOI: 10.5281/zenodo.14551073

17) W. A. E. Ali, M. I. Ashraf, and M. A. Salamin, "A dual-mode double-sided 4 × 4 MIMO slot antenna with distinct isolation for WLAN/WiMAX applications," Microsystem Technologies, vol. 27, no. 3, pp. 967–983, 2021.

18) Z. Qin, W. Geyi, M. Zhang, and J. Wang, "Printed eight-element MIMO system for compact and thin 5G mobile handset," Electronics Letters, vol. 52, pp. 416–418, 2016.

19) Y. Li, C.-Y. D. Sim, Y. Luo, and G. Yang, "High-Isolation 3.5-GHz 8-Antenna MIMO Array Using Balanced Open Slot Antenna Element for 5G Smartphones," IEEE Transactions on Antennas and Propagation, pp. 1-14, 2019. DOI: 10.1109/TAP.2019.2902751.

20) L. Song and J. Geng, "Analysis and Design of a Dual-polarized Printed Monopole Antenna," IETE Journal of Research, pp. 1-8, 2019.

21) A. Zhao and Z. Ren, "Size Reduction of Self-Isolated MIMO Antenna System for 5G Mobile Phone Applications," IEEE Antennas and Wireless Propagation Letters, vol. 18, no. 1, pp. 152-156, Jan. 2019. DOI: 10.1109/LAWP.2018.2883428.

22) M. Li, Z. Xu, Y. Ban, C. Sim, and Z. Yu, "Eight-port orthogonally dual-polarized MIMO antennas using loop structures for 5G smartphone," IET Microwaves, Antennas & Propagation, vol. 11, no. 12, pp. 1810–1816, 2017.

23) M. Abdullah, A. Altaf, M. Anjum, Z. Arain, A. Jamali, M. Alibakhshikenari, F. Falcone, and E. Limiti, "Future smartphone: MIMO antenna system for 5G mobile terminals," IEEE Access, vol. 9, pp. 91593–91603, 2021.

24) H. S. Abubakar, Z. Zhao, B. Wang, S. H. Kiani, N. O. Parchin, and B. Hakim, "Eight-Port Modified E-Slot MIMO Antenna Array with Enhanced Isolation for 5G Mobile Phone," Electronics, vol. 12, no. 316, pp. 1–11, 2023. [Online]. Available: https://doi.org/10.3390/electronics12020316.

25) K. Wong, C. Tsai, and J. Lu, "Two Asymmetrically Mirrored Gap-Coupled Loop Antennas as a Compact Building Block for Eight-Antenna MIMO Array in the Future Smartphone," IEEE Transactions on Antennas and Propagation, vol. 65, no. 4, pp. 1765-1778, 2017.